

# Solar cycle according to mean magnetic field data

V. N. Obridko,<sup>1★</sup> D. D. Sokoloff,<sup>2★</sup> K. M. Kuzanyan<sup>1,3★</sup>  
B. D. Shelting<sup>1★</sup> and V. G. Zakharov<sup>4★</sup>

<sup>1</sup>*IZMIRAN, Troitsk, Moscow Region 142190, Russia*

<sup>2</sup>*Department of Physics, Moscow State University, Moscow 119992, Russia*

<sup>3</sup>*Department of Applied Mathematics, University of Leeds, Leeds LS2 9JT*

<sup>4</sup>*Institute of Continuous Media Mechanics, Korolyov 1, 614061 Perm, Russia*

Accepted 2005 October 16. Received 2005 October 14; in original form 2005 June 28

## ABSTRACT

To investigate the shape of the solar cycle, we have performed a wavelet analysis of the large-scale magnetic field data for 1960–2000 for several latitudinal belts and have isolated the following quasi-periodic components:  $\sim 22$ , 7 and 2 yr. The main 22-yr oscillation dominates all latitudinal belts except the latitudes of  $\pm 30^\circ$  from the equator. The butterfly diagram for the nominal 22-yr oscillation shows a standing dipole wave in the low-latitude domain ( $|\theta| \leq 30^\circ$ ) and another wave in the sub-polar domain ( $|\theta| \geq 35^\circ$ ), which migrates slowly polewards. The phase shift between these waves is about  $\pi$ . The nominal 7-yr oscillation yields a butterfly diagram with two domains. In the low-latitude domain ( $|\theta| \leq 35^\circ$ ), the dipole wave propagates equatorwards and in the sub-polar region, polewards. The nominal 2-yr oscillation is much more chaotic than the other two modes; however the waves propagate polewards whenever they can be isolated.

We conclude that the shape of the solar cycle inferred from the large-scale magnetic field data differs significantly from that inferred from sunspot data. Obviously, the dynamo models for a solar cycle must be generalized to include large-scale magnetic field data. We believe that sunspot data give adequate information concerning the magnetic field configuration deep inside the convection zone (say, in overshoot later), while the large-scale magnetic field is strongly affected by meridional circulation in its upper layer. This interpretation suggests that the poloidal magnetic field is affected by the polewards meridional circulation, whose velocity is comparable with that of the dynamo wave in the overshoot layer. The 7- and 2-yr oscillations could be explained as a contribution of two sub-critical dynamo modes with the corresponding frequencies.

**Key words:** Sun: activity – Sun: magnetic fields – sunspots.

## 1 INTRODUCTION

The basic shape of the solar activity cycle can be described as propagation of the activity wave presented by sunspots from middle solar latitudes to the solar equator. The physical nature of the activity waves is attributed to a dynamo acting somewhere inside (or just below) the solar convective zone. A deeper understanding of the solar cycle presents it as a more complicated phenomenon that involves all latitudes, various waves propagating equatorward as well as polarward, etc. An extended scheme of the solar cycle is based

on the whole bulk of solar activity data rather than on sunspot data alone. Until now, the dynamo models of the solar cycle consider sunspot data as the most informative proxy for the solar activity. It looks promising to enlarge the observational basis of the solar dynamo theory and involve other solar activity data into confrontation with dynamo theory.

The aim of this paper is to involve into a systematic confrontation with dynamo theory the available bulk of data concerning large-scale field on the solar surface.

We start with explanation of the very concept of large-scale magnetic field. The point is that the solar observational astronomy and solar dynamo theory use this wording in quite different senses. The dynamo theory deals with large-scale (mean) magnetic field deep inside the solar convective zone. According to the available dynamo models, this field is preferably toroidal. On the solar surface,

\*E-mail: obridko@izmiran.rssi.ru (VNO); sokoloff@dds.srcc.msu.ru (DDS); kuzanyan@maths.leeds.ac.uk (KMK); shelting@izmiran.rssi.ru (BDS); victor@icmm.ru (VGZ)

the toroidal component of the mean magnetic field is traced by sunspots which cover but a small part of the solar surface. The area on the solar surface remote from sunspots and active regions contains a magnetic field as well. The large-scale component of this field is basically poloidal. Its generation is connected with the poloidal component of the mean magnetic field deep inside the convective zone; however one has to be careful with direct identification of these fields. In any case, we are dealing with the large-scale magnetic field as it is presented on the solar surface.

## 2 OBSERVATIONAL SITUATION

The phenomenon of meridional drift, or more precisely, the displacement of the zones of solar activity in latitude, was revealed virtually simultaneously with the discovery of solar cyclicity. While we recognize Schwabe's report of 1843 as the first indication of a possible 10-yr periodicity, we can find the first statement about the drift of a zone of spots in Carrington's classical treatise of 1863. For a long time, it was considered obvious that both phenomena exhibited a single periodicity.

Now we know that though the spots, indeed, appear at a fixed latitude with a period of 11 yr (or closer to 10 yr in the 20th century), the spot cycle time for each solar cycle is significantly longer. The first spots of a new cycle appear at latitudes of  $40^\circ$  and higher several years before the solar minimum, while the last spots are sometimes observed after the solar minimum at latitudes of about  $5\text{--}10^\circ$ . Thus, the idea of an extended solar cycle was introduced by Harvey (1992).

The next step, namely the analysis of cyclic variations of the large-scale and background fields, was started only in the 1960s. There is no doubt that the periodicity of the large-scale fields at each latitude is close to the periodicity of local fields and sunspots. However, the latitude dependence is less clear. Some authors (Bumba & Howard 1965; Duvall 1979; Howard & LaBonte 1981; LaBonte & Howard 1982; Makarov, Fatianov & Sivaraman 1983; Ulrich et al. 1988; Makarov & Sivaraman 1989; Wang, Nash & Sheeley 1989; Obridko & Gaziev 1992; Komm, Howard & Harvey 1993; Wang, Lean & Sheeley 2000; Ivanov & Obridko 2002) indicate that the meridional drift is directed from the equator towards the poles; however, the others (Perez et al. 1981; Anderson 1984; Lustig & Wohl 1990) contest this. Finally, some papers of the former group (see, e.g. Makarov et al. 1983) admit an additional drift from mid-latitudes towards the equator, along with the meridional drift from the mid-latitudes towards the poles. The inconsistency of these findings is, first and foremost, connected with the difficulties of eliminating the effects of stronger local fields in the total signal. In addition, the solar rotation, whose velocity exceeds that of the meridional drift of the large-scale fields by two orders of magnitude, contributes greatly to Doppler measurements.

The comparatively short interval for which data on the magnetic fields of the entire solar disc are available represents another difficulty. Therefore, the very thorough works by Dikpati & Choudhuri (1995) and Choudhuri & Dikpati (1999) analyse data for only 10 yr, while Wang et al. (2000) consider data for 22 yr.

Obridko & Shelting (2003) studied the meridional drift of the large-scale fields over a long time interval, paying particular attention to the identification of the large-scale fields. The analysis was based on the magnetic field data obtained with various magnetographs over 40 yr and unified into a single data set. Before constructing the latitude–time diagrams, the magnetic field observations at various latitudes were averaged over an entire Carrington rotation.

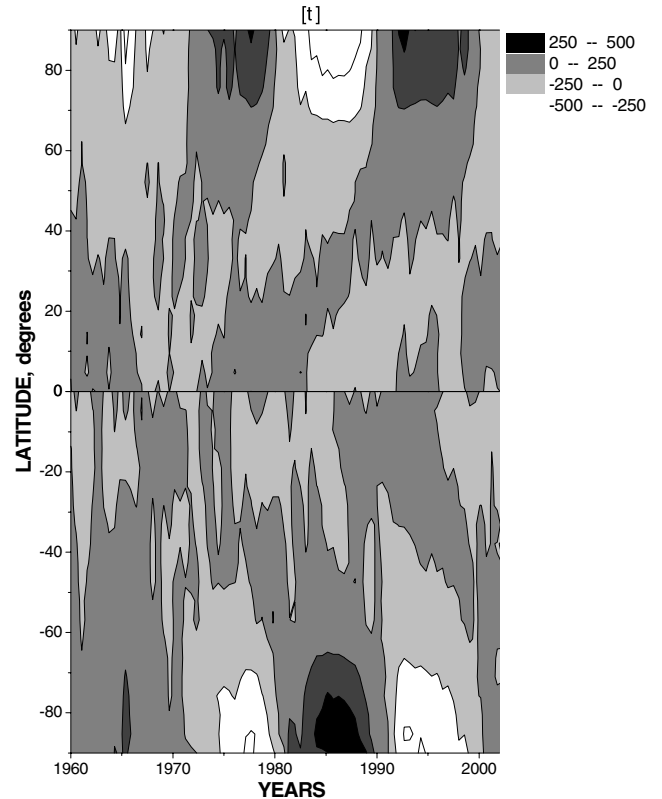


**Figure 1.** Latitude–time diagram for the radial magnetic field calculated in the potential approximation from the magnetograph data. The large-scale magnetic field (vertical axis) is given in  $\mu\text{T}$ ;  $100 \mu\text{T} = 1 \text{ G}$ . Time in years is given in horizontal axis.

The set of data covers 40 yr (1960–2002) and includes the Mt Wilcox magnetic measurements over 1960–1978, Kitt Peak data over 1975–1984 and Stanford measurements from 1976 to the present time. All data were graciously made available by researchers of these observatories. These data were unified into a single Wilcox Solar Observatory system and were used to construct latitude–time diagrams for the radial magnetic fields averaged over a Carrington rotation (Obridko & Shelting 1999). The radial component of the magnetic field in the photosphere was calculated from the detected longitudinal field under potential approximation. A ‘classical’ approximation was used, i.e. the radial field structure was not assumed a priori. Since we were mainly interested in the behaviour of the magnetic field radial component  $B_r$ , we first calculated the daily radial field values for the latitudes from  $0^\circ$  to  $\pm 90^\circ$  in steps of  $1/15$  in the sine of the latitude for the whole time interval. The results were then averaged over a Carrington rotation.

Fig. 1 represents a latitude–time diagram for the radial magnetic field  $B_r$ . The dark grey regions that shade into black near the poles correspond to  $N$  polarity of the magnetic field ( $>0$ ), while the light grey regions that shade into white near the poles correspond to  $S$  polarity ( $<0$ ).

The motion of regions of large-scale magnetic field of each polarity from the equator towards the poles is clearly visible. This drift of the large-scale fields differs fundamentally from the drift of the local fields, in particular, from the motion of the Maunder butterflies from middle latitudes towards the equator. The drift rate of the large-scale fields depends on the latitude. From the equator to latitudes of  $20\text{--}25^\circ$ , the drift is fairly rapid, and the magnetic field passes through this interval in 2–3 yr. At latitudes of  $25\text{--}50^\circ$ , the drift

rate decreases sharply (it does not exceed  $1 \text{ m s}^{-1}$ ), and the magnetic field passes through this  $25^\circ$  interval in 15 yr. Further, the drift rate increases rapidly near the pole, and the magnetic field passes through the remaining  $40\text{--}50^\circ$  in about 1 yr. Thus, the total time for the transport of the large-scale fields is approximately 17–18 yr, i.e. there is an extended cycle. Note that the maximum strength of the local fields is observed in a narrow latitude interval near  $20^\circ$ , whereas the maximum strength of the large-scale fields is observed near the poles. Comparing these large-scale field diagrams with the Maunder butterflies, we arrive at the following conclusions.

(i) There is a clear, mutually opposite motion of the large-scale and local fields: the large-scale fields move from the equator towards high latitudes, while the local fields move from the high latitudes towards the equator. In each activity cycle, the local fields arise before the polarity reversal of the large-scale fields (by 2–3 yr), and disappear near the equator simultaneous with the next polarity reversal of the large-scale fields, covering a time interval of 12–13 yr. The narrow intersection of these two regions occurs at latitude  $20^\circ$ .

(ii) The inclination of the butterflies of the local fields to the time axis is virtually constant during their entire motion from the middle latitudes towards the equator. This inclination is about  $5^\circ$  per year. The local fields are moving over 10–11 yr, from the minimum of each cycle to the minimum of the following cycle. The central area of the butterfly (where there is the greatest number of spots) corresponds to the maximum of the local cycle, and coincides in latitude ( $20^\circ$ ) with the intersection of the diagrams of the local and large-scale fields. The behaviour of the large-scale fields differs from that of the local fields. The drift rate is not constant during the whole time interval, as was indicated above.

Obridko & Shelting (2003) interpret these results as follows. Magnetic fields are generated at the base of the convection zone. The wave of generation moves from mid-latitudes to the equator. The rapidly emerging concentrated local fields follow the wave of generation and form a butterfly diagram. On the other hand, the slowly emerging diffuse large-scale fields loose connection with the wave of generation and are driven to the poles by the meridional drift.

### 3 WAVELET RECONSTRUCTION OF BUTTERFLY DIAGRAM

We have investigated the large-scale magnetic field data for 1960–2000, i.e. for almost two 22-yr cycles. The time dependence of the large-scale magnetic field is presented in Fig. 2.

Basing on Fig. 2, we conclude that a 22-yr cycle is visible on some of the plots presented; however the data are quite noisy. Obridko & Shelting (2003) plotted a butterfly diagram based on these data directly. The butterfly diagram appears to be very noisy as well, and it should be improved to allow reliable conclusions concerning the underlying properties of solar cycles.

Below, we provide the improvement required based on the wavelet technique (see, e.g. Frick et al. 1997). The idea of the method can be described as follows. Let us consider the time-series for each latitudinal belt as a combination of oscillations with various periods. Then, we investigate their energy spectrum for each latitudinal belt separately and isolate frequencies that give main contributions to the signal at a given latitude. If the contributions are from a few frequencies only (it appears that three frequencies give the main contribution), we isolate the spectral intervals near the preferable frequencies. Then, an inverse transform gives us a smoothed integral signal responsible for each spectral band separately. The harmon-

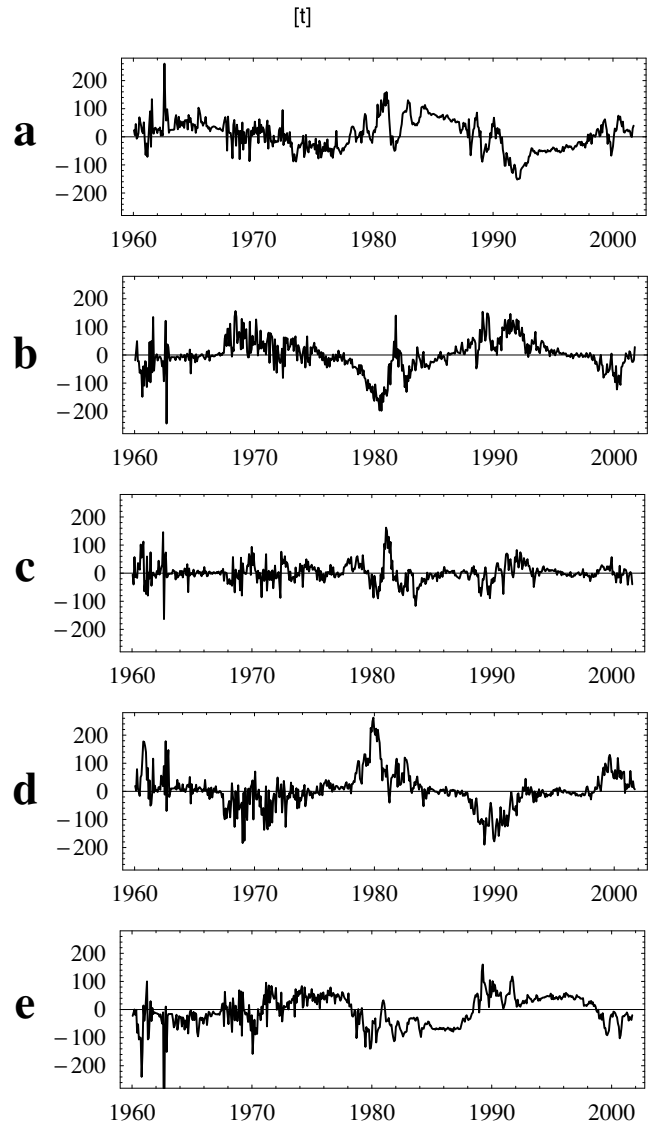


**Figure 2.** Time-series for large-scale magnetic field for various latitudes. (a)  $\theta = -56^\circ$ ; (b)  $\theta = -17^\circ$ ; (c)  $\theta = 0^\circ$ ; (d)  $\theta = 17^\circ$  and (e):  $\theta = 56^\circ$ . The large-scale magnetic field (vertical axis) is given in  $\mu\text{T}$ ;  $100 \mu\text{T} = 1 \text{ G}$ . Time in years is given in horizontal axis.

ics located beyond the spectral bands are considered as noise and excluded from further analysis.

In principle, one could use Fourier transform as a mathematical tool for the data smoothing. In this case, the signal is compared with a harmonic sinusoidal signal of constant amplitude. We know, however, that two neighbouring solar cycles can have different amplitudes, while the Fourier analysis prescribes them a uniform amplitude. As a result, smoothing by Fourier analysis can insert unphysical details into the shape of the signal. It is better to compare the signal with a wave packet of a given frequency. Such packets are known as wavelets. That is the main idea of the wavelet analysis.

Choosing a proper shape of the wave packet  $\psi(t)$ , one can adopt the wavelet analysis to reveal the properties of the signal important to the particular research. Here, we have used the so-called Morlet wavelet, i.e.  $\psi(t) = \exp(2\pi i t - t^2/2)$  which is addressed in the first line to isolate relatively long trains of oscillations with more or less stable frequency rather than to optimize the determination of their

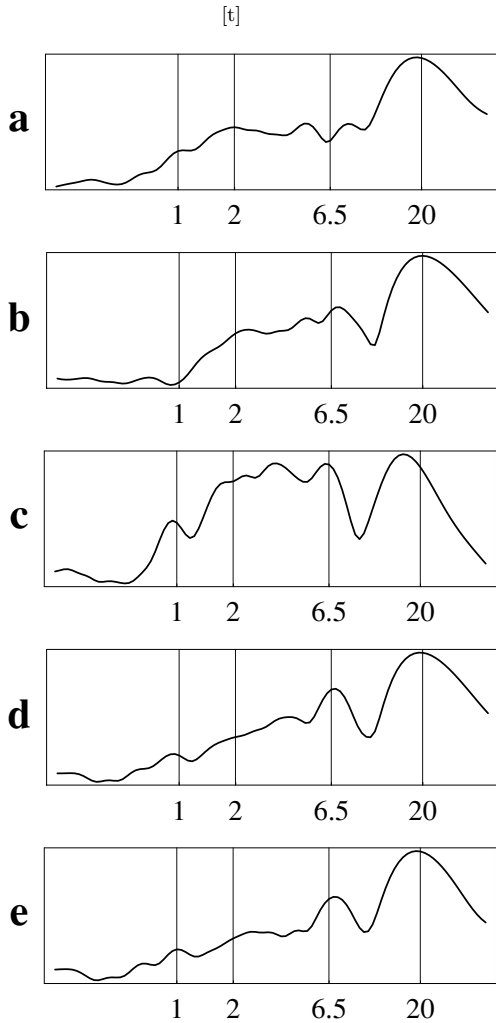


**Figure 3.** Wavelet spectra for various latitudes. (a)  $\theta = -56^\circ$ ; (b)  $\theta = -17^\circ$ ; (c)  $\theta = 0^\circ$ ; (d)  $\theta = 17^\circ$  and (e)  $\theta = 56^\circ$ .

exact location in time. It has better spectral resolution than other well-known wavelets, e.g. the Mexican hat.

The wavelet spectra for various latitudes are illustrated in Fig. 3. The spectra are produced by summation of square of wavelet coefficients. The log-log axes were used. The horizontal axis shows time-scales in years.

We conclude from Fig. 3 that the data under analysis can be decomposed into three spectral bands, which correspond to the following cycle durations: (i) 18–22 yr, (ii) 5.5–7.5 yr and (III) 1.5–2.5 yr.

The contribution from the spectral band I is dominant in most latitudinal belts. Exceptions are the latitudes  $\theta = \pm 30^\circ$  where the nominal 22-yr oscillation is almost absent. One may notice that 7-yr cycle is better visible in the Northern hemisphere at positive latitudes rather than negative ones. This question is not studied in the framework of our paper, and to find out how significant this observational fact is, one may carry out further more-focused studies.

Now, we perform an inverse wavelet transform for each spectral band separately and combine data for various latitudinal belts to obtain butterfly diagrams for each spectral band separately (Fig. 4).

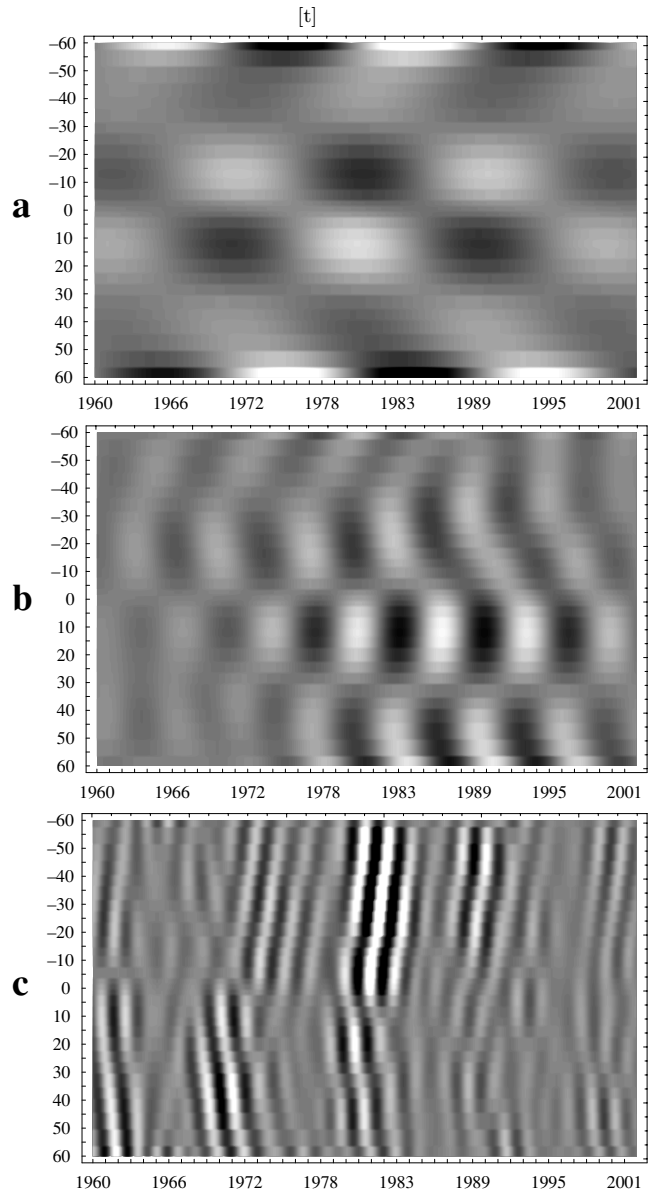


**Figure 4.** Smoothed butterfly diagrams for three spectral bands: (a) spectral band I (18–22 yr); (b) spectral band II (5.5–7.5 yr) and (c) spectral band III (1.5–2.5 yr).

#### 4 DYNAMO INTERPRETATION

From the viewpoint of the dynamo theory, the most intriguing feature in the butterfly diagrams obtained is the fact that the 11-yr oscillation is presented by an almost standing wave. The standard dynamo models of solar activity describe 22-yr cycle as a travelling dynamo wave, which propagates from the mid-latitude domain equatorwards. The direction of the dynamo wave propagation is determined by the sign of the so-called dynamo number, which gives the dimensionless amplitude of the dynamo drivers, i.e. the differential rotation and helicity. This explanation originates in the seminal paper by Parker (1955). This interpretation is reconsidered by Kitchatinov (2002) who suggests that the main direction of the dynamo wave propagation is radial, and the visible equatorial propagation of the wave of sunspot activity is rather minor effect visible because of the observation conditions. For a domain of governing

parameters, Moss et al. (2004) demonstrate that Parker's migratory dynamo produces a standing rather than a travelling wave. In any case, however, both magnetic field components participating in the dynamo wave demonstrate a similar space–time pattern. What about the observation under discussion, the toroidal and poloidal magnetic fields demonstrate two different space–time patterns (travelling and standing waves, respectively). It is worth noting that Durney (1988) in his expansion of solar radial magnetic field data also found signatures of standing waves (see his fig. 2).

We believe that a reasonable explanation of observations is the involvement of a meridional circulation. Suppose that the meridional circulation  $v_b$  is equatorwards at the base of the convective zone and polewards near the solar surface  $v_s$ , at least from the equator up to high latitudes. For the sake of simplicity, we accept that  $v_s = -v_b = v$ . Let the dynamo wave propagate in comoving frame with a velocity  $v_d$ . Then, the velocity of the toroidal field advection is  $V_b = v_d - v$ , while the advection velocity of the poloidal field near the solar surface is  $V_s = v_d + v$ . According to the observations,  $V_s \approx 0$  while  $V_b \approx 4^\circ \text{ yr}^{-1}$  (for the sake of definiteness, we use angular units to measure distances in the meridional direction). It means that  $v_d \approx v \approx 2^\circ \text{ yr}^{-1}$ . We used here a very crude assumption of an equal velocity for the surface and bottom meridional flow for illustrative purposes only.

Note that the interpretation suggested can be related with the dynamo scenarios of Dikpati & Choudhuri (1994) and Dikpati & Gilman (2001) which are essentially connected with meridional circulation. Though note that numerical simulations of meridional circulation suggest that it may take the form of several cells, both radially and latitudinally (e.g. DeRosa, Gilman & Toomre 2002; Brun, Miesch & Toomre 2004). The same transport effect for the magnetic field can be also obtained if we consider different diffusivities at the upper and lower convection zone. This idea, however, requires numerical check.

As an alternative interpretation, one can consider, e.g. dynamo models for a solar rotation law without meridional flow can produce radial oscillations with equatorwards migration of the toroidal fields at low latitudes and polewards migration of them at high latitudes due to the latitudinal growth of the toroidal field over the cycle (cf. Charbonneau 2005).

The magnetic structure recorded in the 22-yr butterfly diagram has a dipole symmetry in agreement with the sunspot data. A field reversal near the latitudes  $\theta = \pm 30^\circ$  is well pronounced. The sunspot data do not demonstrate a clear field reversal at these latitudes. We conclude that the magnetic tubes in sunspot formation move polewards and the displacement is at least about a dozen degrees. This conclusion agrees with the available understanding of sunspot formation (Caligari, Moreno-Insertis & Schuessler 1995; Caligari, Schuessler & Moreno-Insertis 1998). However, we must keep in mind that the radial field of the surface could be the real tracer of the dynamo, and the local fields are decoupled from the bottom toroidal field (cf. Schüssler 2005). We also hope that future dynamo models will also explain the behaviour of the radial surface field.

The 22-yr butterfly diagram for  $|\theta| > 30^\circ$  looks as a polewards wave in agreement with some dynamo models (see e.g. Belvedere, Kuzanyan & Sokoloff 2000).

The intensity of two other cyclic processes recorded in the data under discussion (about 5–7 yr and 2-yr oscillations) is much lower than that of the nominal 22-yr cycle. That is why we do not consider them as two additional dynamo processes active somewhere in the convective zone of the Sun, though such interpretation is possible in principle. The nominal 7-yr oscillation demonstrates a clear equatorwards wave at lower latitudes and a polewards wave at higher

latitudes. The field configuration is dipole. The magnetic configuration is similar to the poloidal magnetic field associated with the toroidal magnetic field of the nominal 11-yr cycle in Parker's migratory dynamo. It is important to stress that the wavelet analysis of sunspot data undertaken by Frick et al. (1997) does not recognize a 7-yr (as well as 2-yr) oscillation. However, one can compare the periods of oscillations found in this paper with various periodicities found by power-spectra analysis of the solar radial magnetic field data series (Durney 1998).

We believe that these facts could be explained as a presence of a subcritical mode with a period of about 7 yr between dynamo modes. This mode is fitted by a strong toroidal field emerging from the bottom of the convective zone and gives a poloidal magnetic field due to  $\alpha$ -effect. However, the rotation shear is insufficient to produce a substantial newborn toroidal field. A region with the hydrodynamic conditions required seems to exist (according to the helioseismological data) in the middle of the convective zone. We attach the dynamo mode under discussion to this radial domain.

As for the nominal quasi-biennial periodicity, its pattern is quite irregular and demonstrates a polewards wave propagating at all latitudes. We consider this wave to be a subcritical dynamo mode operating near the solar surface (cf. Benevolenskaya 1998). Thus, we have two separate dynamos operating at different depths of the solar convection zone. Suppose, the near-surface dynamo produces no or little latitudinal migration, either due to it being predominantly of  $\alpha^2$ -type or due to strong latitudinal dependence of differential rotation versus radial dependence. Then, in low latitudes, where the radial gradient of differential rotation is positive, the condition of equatorwards migration requires negative  $\alpha$ -effect. However, the poleward meridional circulation brings near the surface this equatorial migrations to standing wave form. Note that in high latitudes, both direction of migration of dynamo and meridional circulation should change for keeping the same standing wave.

## 5 CONCLUSION

Traditionally, the direction of the dynamo wave propagation is considered to be a very important element in confrontation between the solar dynamo theories and observations. Our results show that the very concept of the direction of the activity wave propagation is more complicated than it was supposed earlier and depends on the activity tracer used. Correspondingly, the verification process for solar dynamos needs a critical revision.

## ACKNOWLEDGMENTS

This work was supported by the Russian Foundation for Basic Research (grants no. 04-02-16068, 05-02-16090, 03-02-16384/06-02-16887 and 05-02-39017). The authors would like to thank David Moss for helpful discussions, and anonymous referee for very useful remarks.

## REFERENCES

- Anderson B. N., 1984, *Sol. Phys.*, 94, 49
- Belvedere G. M., Kuzanyan K. M., Sokoloff D., 2000, *MNRAS*, 315, 778
- Benevolenskaya E. E., 1998, *ApJ*, 509, 48L
- Brun A. S., Miesch M. S., Toomre J., 2004, *ApJ*, 614, 1073
- Bumba V., Howard R., 1965, *ApJ*, 141, 1502
- Caligari P., Moreno-Insertis F., Schuessler M., 1995, *ApJ*, 441, 886
- Caligari P., Schuessler M., Moreno-Insertis F., 1998, *ApJ*, 502, 481
- Charbonneau P., 2005, *Living Rev. Solar Phys.*, 2, 2. [Online Article]

- Choudhuri A. R., Dikpati M., 1999, *Sol. Phys.*, 184, 61  
Dikpati M., Choudhuri A. R., 1994, *A&A*, 291, 975  
Dikpati M., Choudhuri A. R., 1995, *Sol. Phys.*, 161, 9  
Dikpati M., Gilman P. A., 2001, *ApJ*, 559, 428  
DeRosa M. L., Gilman P. A., Toomre J., 2002, *ApJ*, 581, 1356  
Duvall T. L., Jr, 1979, *Sol. Phys.*, 63, 3  
Durney B. R., 1998, *Sol. Phys.*, 180, 1  
Frick P., Galyagin D., Hoyt D., Nesme-Ribes E., Shatten K., Sokoloff D., Zakharov V., 1997, *A&A*, 328, 670  
Harvey K. L., 1992, in Harvey K. L., ed., *ASP Conf. Ser. Vol. 27, The Solar Cycle*. Astron. Soc. Pac., San Francisco, p. 335  
Howard R., LaBonte B. J., 1981, *Sol. Phys.*, 74, 131  
Ivanov E. V., Obridko V. N., 2002, *Sol. Phys.*, 206, 1  
Kitchatinov L. L., 2002, *Astron. Lett.*, 28, 626  
Komm R. W., Howard R. F., Harvey J. W., 1993, *Solar Phys.*, 147, 207  
LaBonte B. J., Howard R. F., 1982, *Sol. Phys.*, 80, 361  
Lustig G., Wohl H., 1990, *A&A*, 229, 224  
Makarov V. I., Sivaraman K. R., 1989, *Sol. Phys.*, 119, 35  
Makarov V. I., Fatianov M. P., Sivaraman K. P., 1983, *Sol. Phys.*, 85, 215  
Moss D., Sokoloff D., Kuzanyan K. M., Petrov A., 2004, *Geophys. Astrophys. Fluid Dyn.*, 98, 257  
Obridko V. N., Gaziev G., 1992, in Harvey K. L., ed., *The Solar Cycle*. ASP Conf. Ser. Vol. 27, Astron. Soc. Pac., San Francisco, p. 410  
Obridko V. N., Shelting B. D., 1999, *Sol. Phys.*, 184, 187  
Obridko V. N., Shelting B. D., 2003, *Astron. Rep.*, 47, 333  
Parker E., 1955, *ApJ*, 121, 491  
Perez Garde M., Vazquez M., Schwan H., Wohl H., 1981, *A&A*, 93, 67  
Schüssler M., 2005, *Astron. Nachr.*, 326, 194  
Ulrich R. K., Boyden J. E., Webster L., Padilla S. P., Snodgrass H. B., 1988, *Sol. Phys.*, 117, 291  
Wang Y.-M., Nash A. G., Sheeley N. R., 1989, *ApJ*, 347, 529  
Wang Y.-M., Lean J., Sheeley N. R., 2000, *Geophys. Res. Lett.*, 27, 505

This paper has been typeset from a  $\text{\TeX/L\TeX}$  file prepared by the author.